Enhanced Reduction of Cr(VI) by Direct Electric Current in a Comminated Clay

ARTICLE *in* ENVIRONMENTAL SCIENCE AND TECHNOLOGY · MARCH 2004

Impact Factor: 5.33 · DOI: 10.1021/es034578v · Source: PubMed

3 AUTHORS, INCLUDING:

Sibel Pamukcu
Lehigh University
97 PUBLICATIONS **551** CITATIONS

SEE PROFILE

Environ. Sci. Technol. **2004**, *38,* 1236−1241

Enhanced Reduction of Cr(VI) by Direct Electric Current in a Contaminated Clay

SIBEL PAMUKCU,*,† ANTOINETTE WEEKS,‡ AND J. KENNETH WITTLE§

Department of Civil and Environmental Engineering, 13 East Packer Avenue, Fritz Engineering Laboratory, Lehigh University, Bethlehem, Pennsylvania 18015, Thomas L. Brown Associates, 101 Massachusetts Avenue, N.W., Suite 230, Washington, D.C. 20001, and Electro-Petroleum, Inc., 996 Old School Eagle Road, Wayne, Pennsylvania 19087

The probable relation between diffuse double-layer processes and redox reactions that enhance degradation or conversion of contaminants under an applied electric field were examined in a clay medium. Kaolinite clay, precontaminated with hexavalent chromium, was the test soil medium. Analyte, containing ferrous iron, was transported through the kaolinite clay using direct electric current. The Cr(VI) reduction to Cr(III) was followed by measuring the soil redox potential and pH at discrete locations in the clay bed. The post-test distribution of Cr showed significantly more Cr(III) than Cr(VI) at low to slightly acidic pH distribution ($2 < pH < 6$) in clay. The stoichiometric analyses of measured chromium and iron species concentrations versus the measured redox potentials were compared to Nernst equation predictions of an equivalent aqueous system. An average of +0.37 V shift was measured from the linear Nernstian prediction of cell potential. The applied electric field appeared to provide additional "cathodic current" to drive forth the redox reactions. The redox potential shift was explained by possible overpotential development at the clay−water interfaces due to double-layer polarization under the applied field.

Introduction

Heavy metals continue to pose environmental treats when present in contaminated soils. Cr(VI) is of concern because of the broad range of industrial processes that are sources of Cr(VI) contamination of soil and groundwater (*1, 2*). The persistence of Cr(VI) in these media suggests the continuing need for a variety of suitable techniques of treatment (*2*−*4*). A widely accepted method to reduce the impact of chromium in the environment is to convert Cr(VI) to the less toxic and less mobile Cr(III) (*5*−*10*). Ferrous iron, Fe(II), is a suitable reducing agent over a wide range of pH (*11*), hence injection of excess Fe(II) to a Cr(VI)-contaminated soil can enhance the desired process.

Achieving uniform distribution of a reagent by injection in tight clay soils is often difficult owing to the low hydraulic permeability of these soils. Electrokinetically caused migration of ions in soils is a proven method of transport in tight clay soils (*12*−*16*). The ionic migration is most efficient when the clay is water saturated, but it also takes place in less than saturated states of the clay as long as there is continuity of the water phase through the pore structure. More importantly, when electrical energy is supplied to saturated clay, as in an electrolytic cell, it is possible to bring about nonspontaneous oxidation−reduction reactions that could further enhance the desired results. Faradaic reactions take place on clay particle surfaces when the currents pass in the pathways of their diffuse double layers (*17, 18*). Consequently, the electrokinetic processing of soils may have multiple benefits including directed ion migration (injection) into tight clay formations and electrical supply of energy to drive favorable reduction−oxidation reactions in contaminated clays. Regarding the latter of these two benefits, evidence of enhanced Cr(VI) reduction to Cr(III) by electrokinetics was first reported in 1987 by Banarjee and co-workers (*3*) in field tests at a superfund site in Corvallis, OR.

Background

Reactions of Cr(VI) with Fe(II). Under anoxic conditions and acidic environments, Fe(II) can be the dominant reductant of Cr(VI), as given by the following redox reaction:

$$Cr_2O_7^{2-} + 14H^+ + Fe^{2+} \leftrightarrow 2Cr^{3+} + Fe^{3+} + 7H_2O \quad (1)$$

The potential for the reaction given in eq 1 can be written in the form of Nernst equation as follows:

$$E = E_0 + (2.3RT/6F)\log\{([Cr_2O_7^{2-}][H^+]^{14}[Fe^{2+}]^6)/([Cr^{3+}]^2[Fe^{3+}]^6)\} \quad (2)$$

where E_0 as the standard potential = 0.56 V. In oxygenated systems, the ferrous iron may not have much effect on Cr(VI) reduction, except in acidic environments (pH <3). However, Eary and Rai (*19*) and later Fendorf and Li (*9*) showed that oxidation of Fe(II)(aq) by Cr(VI) is possible in well-aerated systems at high pH conditions. Rai and co-workers (*20*) also showed the formation of a solid phase, known as (Cr,Fe)-$(OH)_3$ solid solutions, with rapid precipitation and dissolution kinetics and lower solubility than $Cr(OH)_3$(s).

Electrokinetic Processes in Clays. Electrokinetic process has emerged as a viable technique for in-situ treatment of contaminated soils since Segall and co-workers (*21*) reported detection of high concentrations of metals and organic compounds in electroosmotically drained water of dredged sludge in 1980. Subsequently, many successful applications of the electrokinetically aided transport of inorganic and organic compounds in soils were demonstrated on pure clay−contaminant mixtures in the laboratory (*15, 22*−*33*).

The electrokinetically aided mass transport is based on well-known electrokinetic processes primarily comprised of electroosmotic advection, electrophoresis, and ion migration in a clay−water−electrolyte system. The formation of electric double layer (diffuse double layer, DDL), and the dynamics of the interfacial planes within DDL are responsible for electroosmosis and electrophoresis (*34*). The interfacial planes that play a role are the inner Helmholtz plane (IHP)—the outer limit of the specifically adsorbed water and ions; the outer Helmholtz plane (OHP)—the outer limit of positively charged ions condensed on the clay particle surface (Stern layer); and the slip plane—where the electrokinetic potential (ζ-potential) is measured.

* Corresponding author phone: (610)758-3220; fax: (610)758-6405; e-mail: sp01@lehigh.edu.
† Lehigh University.
‡ Thomas L. Brown Associates.
§ Electro-Petroleum, Inc.

10.1021/es034578v CCC: $27.50
Published on Web 01/06/2004

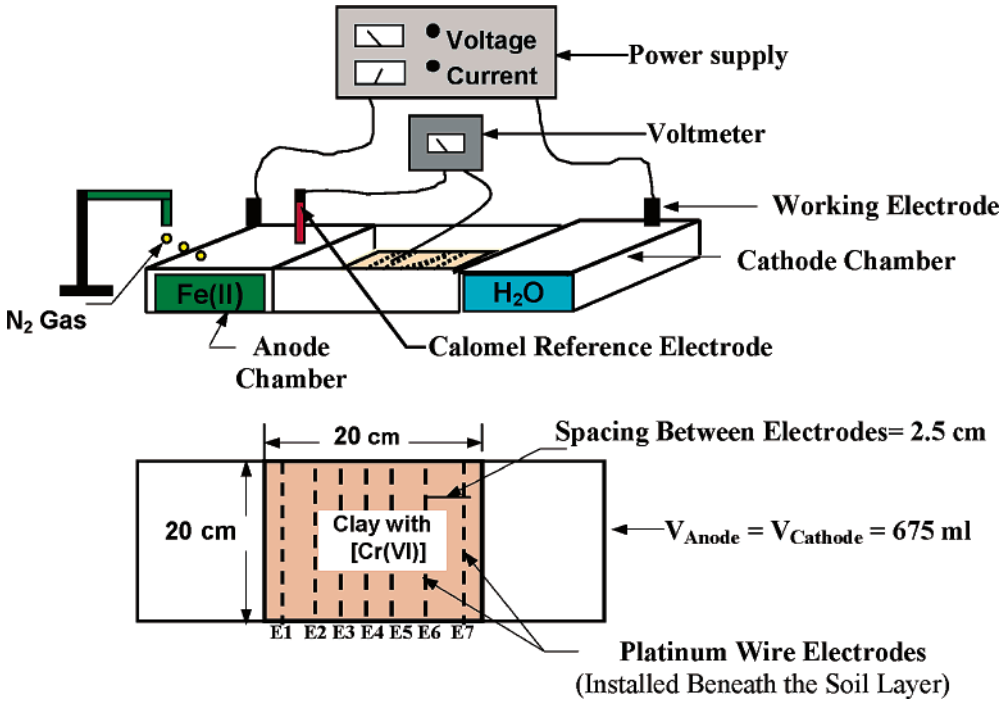

FIGURE 1. Schematic diagram of the modified electrophoretic cell test setup.

Investigation

Treatise of Possible Influence of Electrokinetics on Redox Reactions in Clay. When an external electric field is applied to saturated clay, given the incompatibility between the conductivity of two conducting layers in series, (i) the solid particles with low surface conductivity, and (ii) the surrounding electrolyte solution (pore fluid) with high ionic conductivity, a potential difference occurs across the interface layer (DDL). As a result, the DDL becomes a condenser with a potential difference across its plates (the clay surface and pore fluid boundary), similar to an electrode−specimen interface (*35*). Hence, under external potential, the clay particles can be regarded as a network of electrodes in contact with the pore fluid through a three-dimensional interfacial region, the DDL.

The charge across the plates of the condenser (DDL) can be expressed as (*36*)

$$q^{ddl} = C_{ddl}E_{ddl} \tag{3}$$

where q^{ddl} is the charge (in Coulombs) in DDL; C_{ddl} is the capacitance (in Farads); E_{ddl} is the potential difference (in volts). Clays possess a characteristic surface charge (q^c), and the quantity of counter charge necessary to neutralize this surface is finite; hence, DDL is fully charged at all times ($q^{ddl} = -q^c$). When the ionic concentration in the pore fluid is high, the ions within DDL diffuse and accumulate toward the clay surface, giving rise to concentration polarization. The passage of ions to and from clay surface across DDL represents the Faradaic current. Hence, the current−potential relation arising from concentration polarization can be used for qualitative and quantitative analysis of substances capable of cathodic reduction and anodic oxidation at the clay−water interface (*35*, *36*).

Representing the clay−pore fluid system as two electrical components, a resistor (pore fluid) and a capacitor (DDL) in series, the electrical relationships can be written as

$$E = E_r + E_{ddl} = iR_s + q^{ddl}/C_{ddl} \tag{4}$$

where E is the applied potential across clay−water, E_r ($= iR_s$) is the ohmic potential measured in the resistor R_s (pore water), and i is the current. According to eq 4 with all but C_{ddl} constant, as C_{ddl} varies with ionic concentration, the right-hand side of the equation has to be modified to maintain the equality. The Faradaic current brings about the oxidation−reduction reactions that subsequently maintains the equilibrium within the interface.

In a clay−water−electrolyte system, the diffuse layer becomes compressed at high ionic concentrations, resulting in higher dipole orientation and reduced electrokinetic potential. As the electrokinetic potential is shifted to lower negative values, the potential difference between the IHP and the OHP increase. The electrons transfer across OHP toward the solution, giving rise to "cathodic" current, hence a cathodic reduction in the diffuse layer and its vicinity. The excess potential that causes the cathodic current flow can be interpreted as the "overpotential" (E^*), which a measure of the degree of polarization (*35*). The overpotential essentially represents the surplus of electrical energy necessary to overcome concentration gradients and maintain the electrical equilibrium across the DDL, as given in eq 4. Then considering the overall conversion, the potential difference (E) necessary to drive the redox reaction at a polarizable surface, such as that of clay, can be written as

$$E = E_r + (E_{eq} + E^*) \tag{5}$$

where E_{eq} is described by Nernstian relation (eq 2), and E_r is the ohmic potential across resistor (pore fluid), and $E_{eq} + E^*$ is the new equilibrium potential across the polarized DDL.

Experimental Program

Lehigh Electrophoretic (EP) Treatment Apparatus. A commercially available electrophoretic (EP) (Econo-Submarine Gel Unit, model SGE-020) cell was modified to accommodate the protocols of the desired experiments. Figure 1 shows a schematic of the modified EP cell. The cell is a rectangular translucent box with a square (20 cm × 20 cm) sample tray. There are two liquid chambers on each side of the sample tray and a lid that covers the whole apparatus. The liquid

chambers were used to hold the stock solutions of iron or deionized water. The standard electrophoretic cell was equipped with internal working electrodes. The modified EP cell allowed direct measurement of the redox potential in the soil by use of 0.1 mm diameter platinum wire electrodes embedded in the base plate of the sample tray. Seven wires were stretched transversely at equal intervals (2.5 cm) along the length of the base plate. These electrodes were labeled as E1−E7 starting from the anode end, as shown in Figure 1. Smooth groves cut into the base plate were used to house and secure the platinum wires.

A thin (~2 mm) uniform layer of clay paste containing the reacting agent, Cr(VI), was spread over the electrode wires. The thickness of the clay paste was kept small to achieve as uniform distribution of charges and current on the soil cross section (0.2 cm × 20 cm) as possible. A Calomel reference electrode (Corning Calomel Reference Electrode model 476350, saturated KCl filling) was located in the anode chamber, close to the working electrode. The redox potentials were measured at each platinum wire electrode with reference to the Calomel electrode.

Compressed fiberglass wool pads, 20 cm × 2 cm surface area and 2 mm thick, were used on both sides as "liquid wicks" to help transport the migrating ions from the analyte to the clay and vice versa. The levels of the liquids in the anode and cathode chambers were kept slightly below that of the clay in the sample tray to avoid flooding of the soil cell with excess liquid. Setting the liquid levels as such required an approximate volume of 675 mL of water in each chamber. The edges of the wicks were shredded, immersed into the liquid at one end, and pressed into the clay at the other. The nonconductive, large pore, fiberglass wool pads were intended as interfaces between the soil and the liquid to eliminate electroosmotic flow between the electrode chambers and the clay.

Materials. High-purity (china grade, Ward's Earth Science) kaolinite clay with nominal particle size of 2 μm was used as the test clay medium in all tests. Kaolinite was selected due to its low swelling property and low impurity content to minimize possible influence of background iron and other ions on double-layer interactions. The chromium-contaminated clay samples were prepared by adding freshly mixed potassium dichromate ($K_2Cr_2O_7$) stock solution to dry kaolinite clay at a predetermined molar concentration. The mixture was allowed to equilibrate in a covered container for 24 h. The solid/liquid mass ratio was selected to provide a final water content of 60% by dry weight of the clay, at 100% degree of water saturation. The saturated mass density of the clay paste was measured 1.63 g/cm^3. The initial pH of the mixture was 6.5. The consistency of the resulting moist clay was a soft, smooth paste, allowing for full liquid saturation and uniform distribution of chromium. The paste was transferred into the tray and spread uniformly over the wire electrodes to a thickness of 2 mm. A wire saw with 2 mm thick guiding recess was run over the top of the spread to ensure uniform thickness.

Measured quantities of potassium dichromate ($K_2Cr_2O_7$) and ferrous sulfate ($FeSO_4 \cdot 9H_2O$) were dissolved in deionized water and used as sources of Cr(VI) and Fe(II), respectively. All stock solutions were made from ACS reagent grade materials. The molar concentration of the potassium dichromate solution (mixed with the clay) was kept constant at 0.05 M. The molar concentration of the ferrous sulfate solution supplied at the anode chamber was varied to provide 0.01, 0.04, 0.06, and 0.11 M concentrations of Fe(II) in the analyte for the four separate tests conducted. The initial pH readings of these solutions were 4.9, 4.65, 4.5, and 4, respectively. All Fe(II) stock solutions were deoxygenated with 99.999% ultra purified grade nitrogen gas (N_2) for a minimum of 1 h prior to testing. In all tests, the Fe(II) solution was placed in the anode chamber, while deionized water was used in the cathode chamber.

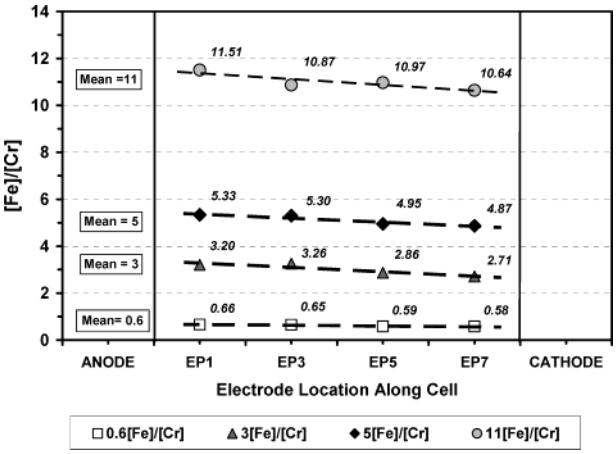

FIGURE 2. Post-treatment distribution of total iron to total chromium ratio (Fe/Cr) in the clay. (Sample ID is based on the average uniform Fe/Cr ratios designated on the graph).

Procedures and Analysis. A constant potential of 5.0 V was applied across the working electrodes for a 24-h duration in all tests. The low 5.0 V potential was selected to remain within the linear range of the power supply used and also prevent excessive gas generation by electrode reactions. The 24-h duration was selected to allow adequate time for uniform distribution of iron in the clay based on previously demonstrated results (*12*, *25*). At the end of each test, water samples were collected from the electrode chambers, and soil samples were collected only above four of the seven wire electrodes at the alternating sites of E1, E3, E5, and E7. An early decision was made to sample at alternate electrode locations rather than all to avoid sampling disturbance and, hence, the possible redistribution of water and ionic constituents at close proximity of the sampling sites. Redox potential and current readings were taken at time intervals at these alternate soil electrodes. The soil and water samples were analyzed for total chromium, hexavalent chromium, total iron and ferrous iron concentrations, and pH.

All soil and liquid samples were collected, preserved, extracted, and diluted in accordance with the approved, standardized U.S. EPA guideline (*37*). The iron and chromium analysis were conducted using a Perkin-Elmer AAnalyst 100 flame atomic absorption spectroscopy (AA) and a Hach DR/4000U spectrophotometer (UV).

Results and Discussions

Post-test Distribution of Cr(III) and Cr(VI). A set of four tests was conducted with varying Fe(II) concentrations in the anode chamber. As shown in Figure 2, at the end of 24-h treatment, the Fe/Cr ratio distribution remained moderately uniform throughout each sample. This is attributed to retarded chromium transport and uniform distribution of iron across the thin cross-section of the specimen during treatment. The actual measured concentration of each component was used in the stoichiometric calculations, but the average Fe/Cr ratios were used for sample identification. Accordingly, the average Fe/Cr distribution computed as 0.6Fe/Cr, 3Fe/Cr, 5Fe/Cr, and 11Fe/Cr designated each of the four tests, respectively.

One control test was conducted to assess the migration of chromium out of clay and the migration of iron into the clay in the absence of an applied electric field. The diffusive transport through the fiberglass wool wicks resulted in less than 2% of the total chromium migration into the anode and cathode chambers and less than 5% of the total iron (at highest

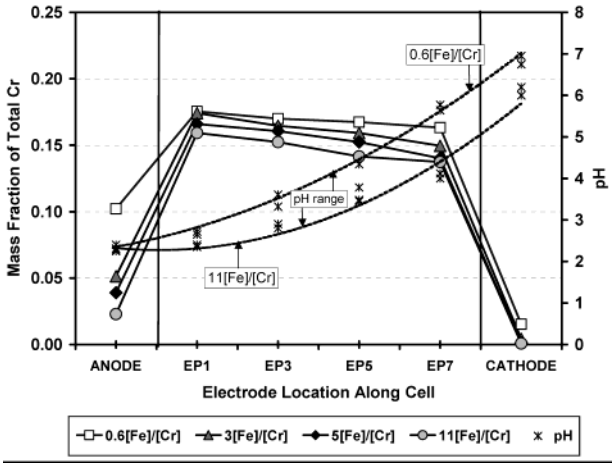

FIGURE 3. Post-treatment distribution of total chromium in soil and the electrode chamber liquids.

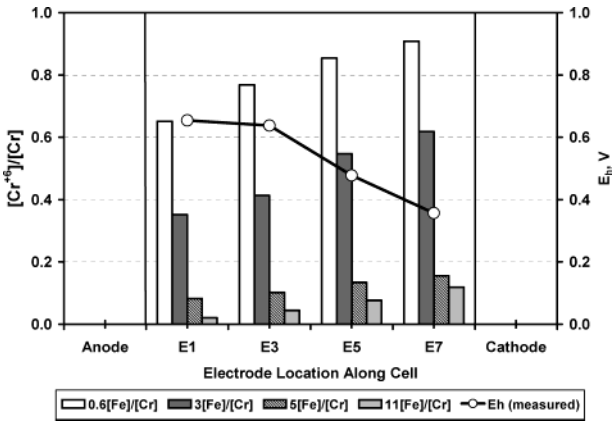

FIGURE 4. Mass fraction distribution of Cr(VI) based on total chromium measured at each electrode location.

concentration application of 0.11 M in anode) migration into the clay within 24-h duration.

Figure 3 shows the post-treatment distribution of total chromium at each soil electrode (platinum wires) and the power electrode chambers, normalized by the initial total mass of chromium in soil. The pH distributions obtained for all test samples are superimposed onto this graph. The trend lines outline the lower and upper bounds of the measured pH values.

As observed, the post-test mass fraction distribution of chromium remained fairly uniform in all the soil samples from the anode to the cathode side. The percentage of total chromium retained in the soil decreased at higher Fe concentrations owing to lower soil pH values. As Cr(VI) is likely to be retained on soil by adsorption at low pH (~40% on kaolinite at pH <4.5; *38*), the adsorption of Cr(III) is less than 10% at those pH values (*39*). Therefore, at or below pH 5, most of the aqueous Cr(III) species available in the pore space would have migrated to the cathode chamber where it would likely precipitate into its trihydroxide solid-phase $Cr(OH)_3$ or other polynuclear hydroxide complexes (*20*, *40*).

Formation of solids was evident by the "brownish" color precipitates, and also less than 10^{-4} M concentrations of aqueous Cr were observed in the cathode chamber liquid at the completion of testing. One complicating factor in speciation analysis was inadequate post-test sampling of these solids from the cathode chamber. This is believed to have introduced an error in the mass balance calculations of the Cr and Fe as well. There is approximately 20−38% of the total chromium unaccounted for in low to high Fe-content

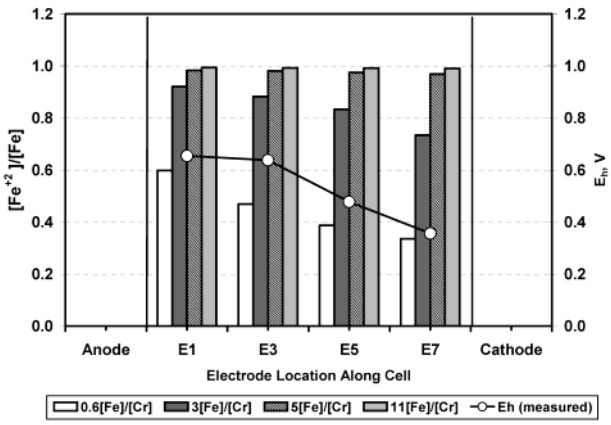

FIGURE 5. Mass fraction distribution of Fe(II) based on total iron measured at each electrode location.

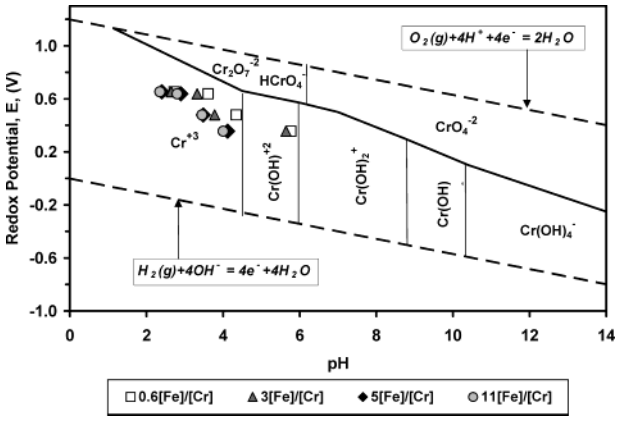

FIGURE 6. Test data superimposed on *E*−pH stability field diagram (*41*).

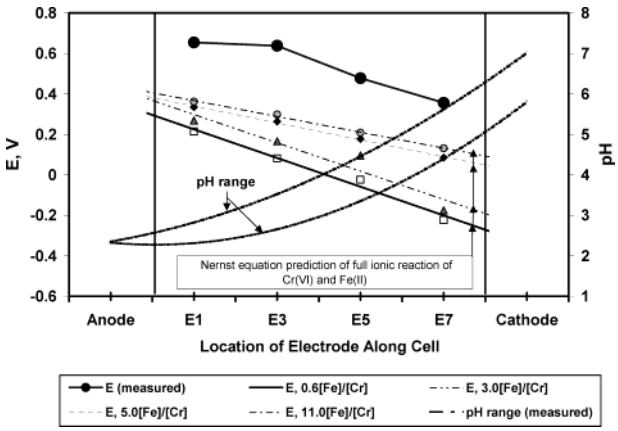

FIGURE 7. Distribution of predicted redox potential of an equivalent aqueous system based on measured concentrations of components at each electrode location.

specimens, respectively. Similarly, mass balance errors from 50 to 55% were calculated for total Fe, which is also attributed to inadequate sampling of solids in cathode chamber.

Figure 4 presents the concentration distribution for Cr(VI) normalized by the total Cr measured at each soil electrode. The Cr(VI) fraction decreases toward the anode, which is indicative of preferential migration of $Cr_2O_7^{2-}$ into the anode chamber. Approximately 10% of the total chromium migrated into the anode chamber liquid. The opposite trend is true for Cr(III), as the aqueous cationic species tend to migrate into the cathode chamber. Monomeric hydroxide complexes of Cr(III) would remain stable in solutions at the pH levels

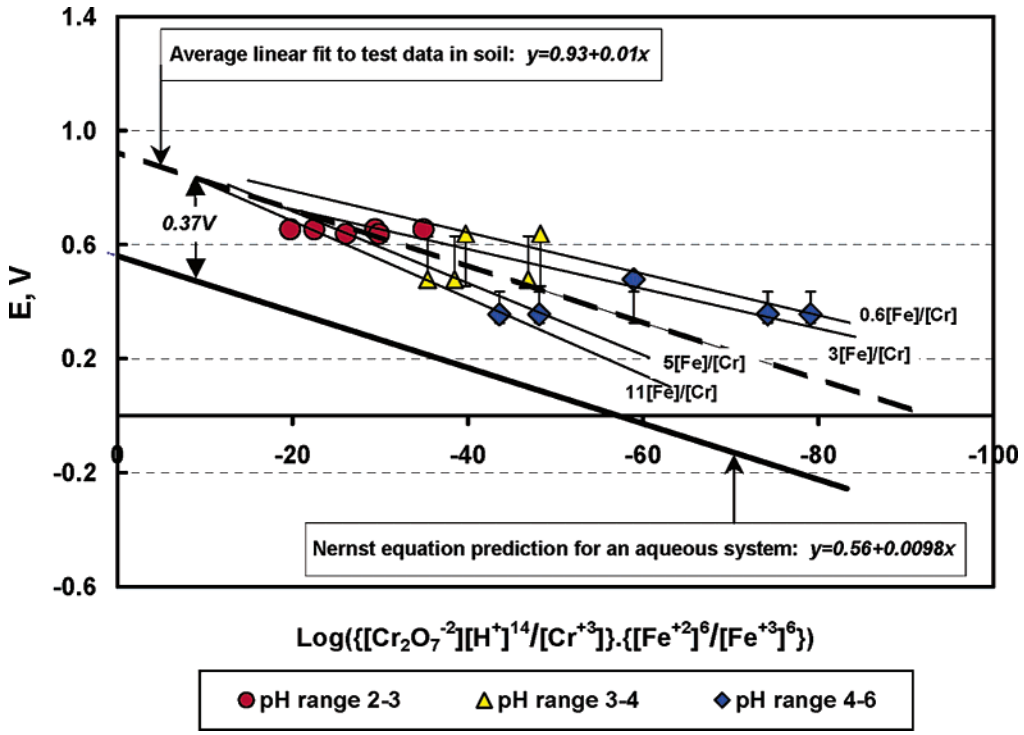

FIGURE 8. Measured and predicted redox potential variation with reaction quotient of measured species concentration in Nernst relation.

encountered in the region of the anode, but above pH 4 they hydrolyze to form polynuclear complexes and ultimately precipitate from solution (*40*).

Figure 5 shows the distribution of normalized Fe(II). A fraction of Fe(III) remaining in the clay and the portion that migrated into the cathode chamber is likely to be bound in hydroxide solids precipitated as $(Cr,Fe)(OH)_3$ and $Fe(OH)_3$ at pH levels higher than 3. The unaccounted Fe was probably bound in these solid compounds, which were not adequately sampled as discussed above. Although the tests were initiated under anoxic conditions, the electrolysis of water at the anode produces O_2(g) and inevitably oxidizes part of the available Fe(II) in that chamber. Therefore, it is also plausible that a portion of the Fe initially driven into the soil was already in the form of Fe(III).

Redox Potential Measurements. Superimposed in Figures 4 and 5 are the redox potentials measured at the soil electrodes E1, E3, E5, and E7. The measured redox potential value (*E*) at each electrode location varied slightly for all tests such that one standard deviation bar was smaller than the marker used at each measurement point in Figures 4 and 5. The current density maintained in the range of 0.09−0.1 mA/cm^2 after about 1 h of treatment. Similarly, the redox potential measurements maintained a nearly constant value after about 1 h of treatment for all but the first (E1) electrode close to the anode chamber. The redox potential measured beyond the first hour was averaged over time at each electrode.

The redox measurements in soil showed the trend of oxidizing to reducing conditions from anode toward cathode, respectively. The *E* and pH measurements for each sample were superimposed on a stability field diagram (*41*) for chromium, as shown in Figure 6. Since predictions from stability diagrams are only accurate when the system approaches thermodynamic equilibrium, the plot is not intended to verify but rather show the dominance of Cr(III) species at the recorded *E* and pH measurements. This representation may particularly be important for confirmation of the process for technology development since speciation of metals and their stability as measured by their solubility influences the use of most in-situ technologies for remediation purposes.

The equilibrium cell potential for an aqueous system was calculated at each electrode using the Nernst relation given in eq 2. The calculated values also showed the oxidizing to reducing trend from anode to cathode, as given in Figure 7. The measured potential was compared to the computed *E*, by plotting them against the reaction quotient (*Q*) of eq 2. This comparison is shown in Figure 8. The data were grouped to represent common pH ranges and Fe/Cr ratios for the four test sets. The average linear fit to the overall data was essentially parallel (slope = 0.01) to the Nernstian prediction (slope = 0.0098), with an approximate constant potential shift of +0.37 V. The standard deviation of the redox potential shift from the equilibrium value was 0.05V. This positive shift from equilibrium potential is indicative of the cathodic overpotential generated due to the applied electric field, as discussed under the Investigation section previously.

The low pH range (pH 2−3) data showed the best agreement with the linear fit. The scatter at higher pH values can be attributed to the influence of pH on DDL interactions. Overpotential increases with the current density across the OHP and therefore with the degree of polarization on the electrode surface. At low pH, the DDL is compressed with a high degree of polarization; therefore, the overpotential is close to maximum as the measured values tend to cluster with little deviation from the mean value. At higher pH, the DDL is expanded with reduced degree of polarization; consequently, the overpotential is expected to decrease. Yet, the diffuse layer ions are now less restricted to move; therefore, discernible fluctuations are likely to occur in potential development across the OHP interface, where the cathodic current is diffusion controlled.

Literature Cited

(1) Palmer, C. D.; Puls, R. W. *EPA Groundwater Issue*; EPA/540/5-94/505; Office of Solid Waste and Emergency Response, U.S. EPA: Washington, DC, 1994; 12 pp.

(2) Batchelor, B.; Schlautman, M.; Hwang, I.; Wang, N. *Kinetics of Chromium(VI) Reduction by Ferrous Iron*; ANRCP-1998-13; Amarillo National Resource Center for Plutonium, U.S. DOE: Amarillo, TX, September 1998; 15 pp.

(3) Banerjee, S.; Horng, J.; Ferguson, J. F.; Nelson, P. O. *Field Scale Feasibility Study of Electrokinetic Remediation*; CR811762-01;

Risk Reduction Engineering Laboratory, Office of Research and Development, U.S. EPA: Cincinnati, OH, 1987; 129 pp.
(4) Lingren, E. R.; Hankins, M. G.; Mattson, E. D.; Duda, P. M. *Electrokinetic Demonstration at the Unlined Chromic Acid Pit*; SAND97-2592.UC-602; Sandia National Laboratories, U.S. DOE: Sandia, NM, 1998; 143 pp.
(5) Bartlett, R. J.; Kimble, J. M. *J. Environ. Qual.* **1976**, *5* (4), 383−386.
(6) Eary, L. E.; Rai, D. J. *Environ. Sci. Technol.* **1988**, *22*, 972−977.
(7) Anderson, L. D.; Kent, D. B.; Davis, J. A. *Environ. Sci. Technol.* **1994**, *28*, 178−185.
(8) Powell, R. M.; Puls, R. W.; Hightower, S. K.; Sabatini, D. A. *Environ. Sci. Technol.* **1995**, *29*, 1913−1922.
(9) Fendorf, S. E.; Li, G. J. *Environ. Sci. Technol.* **1996**. *30*, 1614−1617.
(10) Kozuh, N.; Stupar, J.; Gorenc, B. J. *Environ. Sci. Technol.* **2000**, *34*, 112−119.
(11) Buerge, I. J.; Hug, S. J. *Environ. Sci. Technol.* **1997**, *31*, 1426−1473.
(12) Pamukcu, S.; Wittle, J. K. *Environ. Prog.* **1992**, *11*, 241−250.
(13) Probstein, R. F.; Hicks, R. E. *Science* **1993**, *260*, 498−503.
(14) Lageman, R. *Environ. Sci. Technol.* **1993**, *27*, 2648−2650.
(15) Acar, Y. B.; Alshawabkeh, A. N. *Environ. Sci. Technol.* **1993**, *27*, 2638−2650.
(16) Acar, Y. B.; Alshawabkeh, A. N. *J. Geotech. Eng.* **1996**, *122* (3), 173−185.
(17) Grahame, D. C. *J. Electrochem. Soc.* **1951**, *98*, 343.
(18) Grahame, D. C. *J. Electrochem. Soc.* **1952**, *99*, 370C.
(19) Eary, L. E.; Rai, D. *Soil Sci. Soc. Am.* **1991**, *55*, 676−683.
(20) Rai, D.; Sass, B. M.; Moore, D. A. *Inorg. Chem.* **1987**, *26*, 345−349.
(21) Segall, B. A.; O'Bannon, C. E.; Matthias, J. A. *J. Geotech. Eng.* **1980**, *106* (10), 1148−1152.
(22) Bruell, C. J.; Segall, B. A.; Walsh, M. T. *J. Environ. Eng.* **1992**, *118*, 1, 68−83.
(23) Runnells, D. D.; Wahli, C. *Ground Water Monit. Rem.* **1993**, *13* (1), 121−129.
(24) Acar, Y. B.; Alshawabkeh, A. N.; Gale, R. *J. Waste Manage.* **1993**, *13*, 141−151.
(25) Wittle, J. K.; Pamukcu, S. *Electrokinetic Treatment of Contaminated Soils, Sludges, and Lagoons*; Final Report DOE/CH-9206; Argonne National Laboratory, U.S. DOE: Argonne, IL, 1993; 45 pp.
(26) Shapiro, A. P.; Probstein, R. F. *Environ. Sci. Technol.* **1993**, *27*, 283−291.
(27) Eykholt, G. R.; Daniel, D. E. *J. Geotech. Eng.* **1994**, *120* (5), 797−815.
(28) Hicks, R. E.; Tondorf, S. J. *Environ. Sci. Technol.* **1994**, *28*, 2203−2210.
(29) Shapiro, A. P.; Probstein, R. F.; Hicks, R. E. *Geotechnique* **1995**, *45*, 355−359.
(30) Yeung, A. T.; Hsu, C.; Menon, R. M. *J. Geotech. Eng.* **1996**, *122* (8), 666−673.
(31) Reddy, K. R.; Parupudi, U. S.; Devulapalli, S. N.; Xu, C. Y. *J. Hazard. Mater.* **1997**, *55*, 135−158.
(32) Pamukcu, S.; Weeks, A.; Wittle, K. *J. Hazard. Mater.* **1997**, *55*, 305−318.
(33) Pamukcu, S.; Huang, C. P. In *Hazardous and Radioactive Waste Treatment Technologies Handbook*; Chang, H. O., Ed.; CRC Press: Boca Raton, FL, 2001; Chapter 3.
(34) Hunter, R. J. *Zeta Potential in Colloid Science: Principles and Applications*; Academic Press: London, 1981.
(35) Bard, A. J.; Faulkner, L. R. *Electrochemical Methods: Fundamentals and Applications*; John Wiley & Sons: New York, 1980.
(36) Kortum, G.; Bockris, J. O'M. *Textbook of Electrochemistry*; Elsevier: Amsterdam, 1951; Vol. 2.
(37) *Standard Methods for the Examination of Water & Wastewater*, 18th ed.; APHA, AWWA, & WEF: Washington, DC, 1992.
(38) Zachara, J. M.; Girvin, D. C.; Schmidt, R. L.; Resch, T. *Environ. Sci. Technol.* **1987**, *21*, 589−594.
(39) Fendorf, S. E. *Environ. Sci. Technol.* **1994**, *28*, 284−289.
(40) Mertz, W. *Physiol. Rev.* **1969**, *49* (2), 163−232.
(41) Schmidt, R. L. *Thermodynamic Properties and Environmental Chemistry of Chromium*; PNL-4881/UC-11; Battelle Pacific Northwest Laboratories, U.S. DOE: Richland, WA, 1984.

Received for review June 10, 2003. Revised manuscript received November 17, 2003. Accepted November 28, 2003.

ES034578V